

Phenol and Polyphenol Removals in Olive Mill Effluent with Nano-ZnO-Magnetite Composite via Photo Catalysis

Delia Teresa Sponza and Merve Balaban

Department of Environmental Engineering, Dokuz Eylul University, Turkey

Volume 1 Issue 2 - 2019

Received Date: 17 Apr 2019

Accepted Date: 18 May 2019

Published Date: 25 May 2019

2. Keywords

Olive mill effluent; Nano-znO-magnetite composite; Phenol; Tyrosol; Hydroxytyrosol; Photo catalysis

1. Abstract

Olive mill wastewater (OMW) contains high concentration of organic matter, acidic pH values, suspended solids and high content of phenols and polyphenols which are toxic substances. The aim of this study is the removals of total phenol and two polyphenols namely tyrosol and hydroxytyrosol in the OMW by Nano-ZnO-Magnetite composite via photo catalytic degradation. For photo catalytic degradation under UV, with the optimum concentration of Nano-ZnO-Magnetite (3 mg per liter), maximum 75% total phenol yield, 80% and 51% tyrosol and hydroxytyrosol removals was obtained at a irradiation time of 30 minute and at a UV power of 300 W.

3. Introduction

Most researchers concentrated their studies on TiO_2 as photo catalyst compared to the other metal oxides for the degradation of environmental pollutants [1]. ZnO is better because it absorbs large fraction of the solar spectrum and more light quanta than TiO_2 [2]. Researchers have highlighted the performance of ZnO on degradation of some organic compounds [3]. In addition, ZnO has more functions than TiO_2 [4]. Recently, researchers have pointed out that ZnO can also be used in the acidic or alkaline conditions through proper treatment [5]. Furthermore the optimum pH reported for ZnO process is close to neutral value, whereas the optimum pH for TiO_2 mostly lies in acidic region. Hence the ZnO process is more economical for the treatment of industrial effluents. ZnO has been reported to be more efficient than TiO_2 in some processes such as the advanced oxidation of pulp mill bleaching wastewater [6], the photo oxidation of phenol [7] and photocatalysed oxidation 2-phenyl phenol [8]. In particular, ZnO has attracted much attention with respect to the degradation of various pollutants due to its high photosensitivity, stability and wide band gap. While TiO_2 is widely employed as a photo catalyst, ZnO is a suitable alternative to TiO_2 as it has a similar band gap energy (3.2 eV) [9], with larger quantum efficiency. Higher photo catalytic degradation efficiencies of contaminant

dyes have been reported.

Therefore, the aim of this study is the removals of total phenol, and two polyphenols (tyrosol and hydroxytyrosol) in the OMW via photo catalytic processes at increasing 3 mg/L Nano-ZnO-Magnetite concentration at increasing irradiation times (30 min, 60 min, 90 min, 180 min and 240 min) and at pH 4.

4. Materials and Methods

4.1. Synthesis of Nano-ZnO-Magnetite Composite under laboratory conditions

Nanoparticle is produced under laboratory conditions and immobilization method is used for this purpose. The magnetite sample was ground and sieved to 200-mesh size, then is washed with demineralized water for 3–4 times. The slurry of magnetite was prepared in water and it was stirred for 1 h, kept overnight, filtered under vacuum and the resultant solid cake was exposed to slow evaporation till the completely dry material was obtained. 10 g of magnetite was added to a solution containing 2g zinc acetate dihydrate dissolved in 250 ml of N, N-dimethylformamide and the mixture was sonicated for about 3 h in order to obtain homogeneous suspension. To this solution, 100 ml of 0.1 M NaOH/ H_2O solutions was added with constant stirring for 1 h. The Nano composite powder was obtained after successive centrifugation

*Corresponding Author (s): Delia Teresa Sponza, Department of Environmental Engineering, Dokuz Eylul University, Turkey, E-mails: delya.sponza@deu.edu.tr and merve-balaban@gmail.com

and dispersions in alcohol and the solid mass was dried at 75 °C under vacuum incubator for 4 h. Then it is calcinated at 200 °C for 2–3 h in a Muffle furnace. The dried Nano-ZnO-Magnetite Nano composite was then is used for photo catalytic experimentations.

4.2. Analytical Methods

A HPLC Degasser (Agilent 1100), a HPLC Pump (Agilent 1100), a HPLC Auto-Sampler (Agilent 1100), a HPLC Column Oven (Agilent 1100) and a HPLC Diode-Array-Detector (DAD) (Agilent 1100) were used for phenol and 2 polypenol measurements namely tyro sol and hydroxytyrosol determined in the OMW. About 10 mg of a standard of phenolic acids (phenol, tyro sol and hydroxytyrosol) was weighed accurately and they were dissolved into volumetric flasks containing 10 mL 1:1 MeOH/distilled water to obtain stock solutions. For calibration curves, the stock solution was diluted with 1:4 MeOH/distilled water to obtain the concentration sequence. The linear range and the equations of linear regression were obtained through such a sequence of 50 mg/L, 20mg/L, 10 and 5 mg/L. Mean areas generated from the standard solutions were plotted against concentration to establish calibration equations. R^2 values of calibration graphs of caffeic acid, was found as 0.99.

4.3. Photo catalytic reactor and operational conditions

Photo catalytic degradation experiments were carried out in self-designed quartz glass reactors. The dimensions of the reactors were 38 and 3.5 cm and the constant power of the UV lamps was 300 W. The experiments were performed at room temperature and the pH of the reaction mixture was 4. Photo catalytic experiments were carried out with a known quantity of Nano-ZnO-Magnetite (3 mg/l) composite at different irradiations times (30 min, 60 min, 90 min, 180 min and 240 min).

4.4. X-ray diffraction (XRD) Analysis

XRD measurements were carried out with the RIGAKU D-Max 2200 PC. X-ray diffraction were used for the identification of crystalline materials and their structure. Each crystalline solid has its unique characteristic X-ray powder pattern and can be used for the characterization of crystalline properties of materials. Preliminarily, the material was characterized; X-ray crystallography may be used to determine the atom distribution in the crystalline structure and the distance between atoms and angles [10].

4.5. Fourier transform infrared (FT-IR)

FTIR spectra were determined using an Perkin Elmer System with a Spectrum of BX. Fourier transform infrared spectroscopy (FTIR) is a technique which is used to obtain an infrared spectrum of absorption, emission, photoconductivity or Raman scattering of a solid, liquid or gas. FTIR spectrometer catch resolution

with high spectrum data. This advantage of the spectrometer cause determining the intensity of wavelengths [11].

5. Results and Discussion

5.1. X-ray diffraction (XRD) Analysis Results

XRD was used to verify the chemical composition and the crystal structure of Nano-ZnO-Magnetite Nano composite [12]. **Figure 1** represents the XRD pattern of Nano-ZnO-Magnetite core/shell. Considering this figure, it is shown that after coating, we have enhancement in peak intensity which is caused by overlapping of Fe_3O_4 peaks [13]. No peaks corresponding to the impurities are detected, indicating that Fe_3O_4 -ZnO heterostructure were formed during the photo degradation process [14].

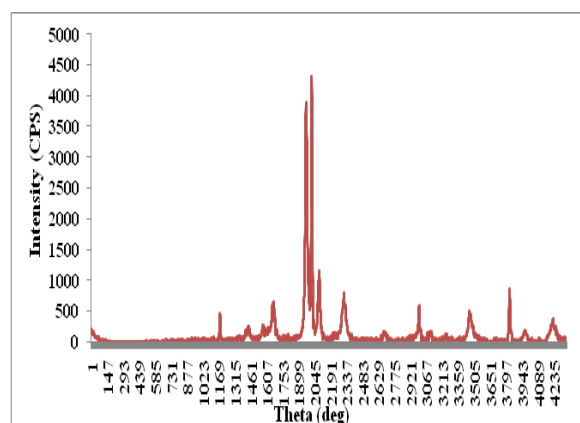


Figure 1: XRD patterns of Nano-ZnO-Magnetite.

5.2. FT-IR Analysis results

Figure 2 shows the FT-IR spectra of Nano-ZnO-Magnetite. A the absorptions at 1395.25/cm and 1591.29/cm are special peaks of the COO-Fe bond. This bond appeared via the hydroxide groups on the outer layer of the magnetite [15]. These peaks reveal that Fe_3O_4 has been successfully immobilized onto the surface of ZnO. Combining the XRD results, it can be concluded that ZnO had been coated on the Fe_3O_4 , successfully. Therefore, crystal form of Nano-ZnO-Magnetite composite converts the amorphous shape. As a result, the peak number in the Nano-ZnO-Magnetite composite decreases in the amorphous shape.

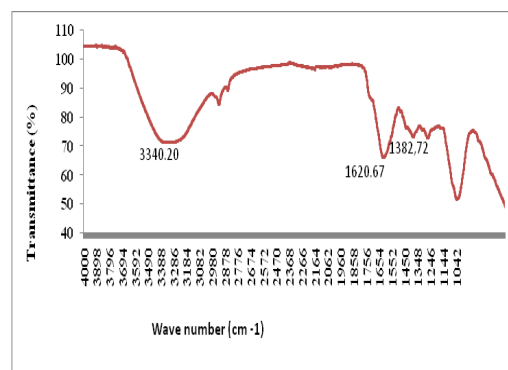


Figure 2: FTIR spectrum of Fe_3O_4 , ZnO, Nano-ZnO-Magnetite and Nano-ZnO-Magnetite .

5.3. Effect of Irradiation times on the Removals of phenol in the OMW

Figure 3 shows the effect of different UV irradiation times (30 min., 60 min., 90 min., 180 min. and 240 min) on photo degradation of phenol at a pH of 4.60 at a temperature of 20 °C after at a 3 g/L concentration of Nano-ZnO-Magnetite Nano composite with an UV lamp with a power of 300 W. From Figure 3 it can be seen that as the irradiation time were increased from 30 min, to 60 min, to 90 min, and to 180 min, the phenol yield increased from 57%, to 63%, to 65%, to 77%, and stabilized to 77%. Further increase of adsorption time to 240 min did not increase the phenol yield. The optimum irradiation time can be considered as 180 min for the maximum removal efficiency of phenol (77%). The percentage of degradation of phenol was 65.5% under UV light after 150 min irradiation time. The phenol degradation was only 52% when pure ZnO was used, which is lower than that in the presence of either Fe₃O₄-ZnO.

5.4. Polyphenol analysis Results

According to the results of chromatograms in HPLC analysis, 112.6 mg/L concentration of hydroxytyrosol and 172.7 mg/L concentration of tyrosol was identified in raw OMW illustrated in Figure 4. In a study investigated by Manouchehr et al., (2014), polyphenols were analyzed in the olive oil mill effluents. 115.9 mg/L and 50.3 mg/L concentration of hydroxytyrosol and tyrosol were found, respectively, and these data are consistent with our. The results showed that hydroxytyrosol and tyrosol were most abundant phenolic compounds in OMW (Figure 4). Hydroxytyrosol and caffeic acid show a powerful antioxidant activities [16]. Hydroxytyrosol inhibits human LDL oxidation, inhibits platelet aggregation and exhibits anti-inflammatory and anticancer properties [17]. Tyrosol showed similar concentrations with hydroxytyrosol in the OMW (Figure 4). Samuel et al. (2008) reported that hydroxytyrosol is very effective in preserving cellular anti-oxidant defenses [18].

By using 3 g/L Nano-ZnO-Magnetite Nano composite with 30 min irradiation time at pH 4 and a temperature of ±20 °C with an UV power of 300 W during photo oxidation. The removal efficiencies of tyrosol and hydroxytyrosol were obtained as 80% and 51%, respectively. Their concentrations decreased from 172.7 mg/L to 34.8 mg/L for tyrosol and from 112.6 mg/L to 55.2 mg/L for hydroxytyrosol, respectively, after treatment with 3 g/L Nano-ZnO-Magnetite Nano composite under 300 W UV irradiation after 30 min irradiation time (Figure 5, Table 1).

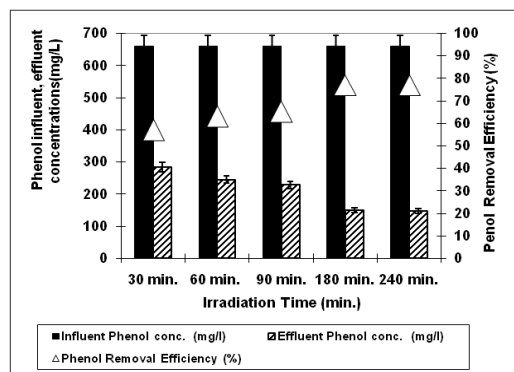


Figure 3: The effect of Irradiation time on phenol yield (Influent Conc.: 660 mg/L, T: ±20 °C, pH: 4.00, Nano-ZnO-Magnetite concentration: 3g/L, UV power: 300 W).

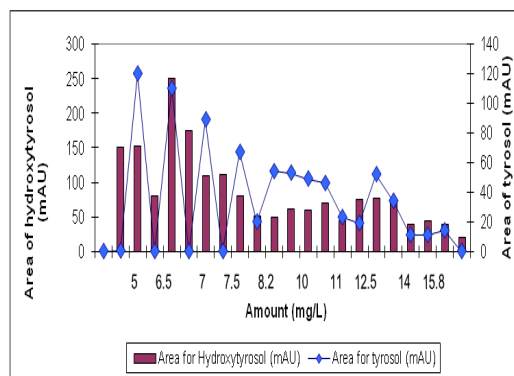


Figure 4: The concentration of tyrosol and hydroxytyrosol found in raw OMW.

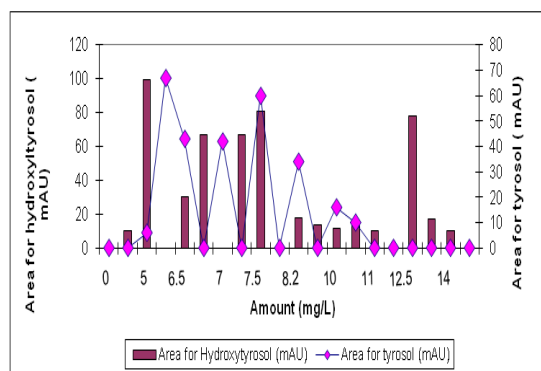


Figure 5: The concentration of tyrosol and hydroxytyrosol found in treated OMW with UV photo oxidation.

Table 1: Removal Efficiencies of polyphenols (tyrosol and hydroxytyrosol) in OMW.

Polyphenols	Raw OMW (mg/L)	Treatment of OMW with UV photooxidation (mg/L)	Removal Efficiency (%)
Tyrosol	172.7	34.8	80
Hydroxytyrosol	112.6	55.2	51

References

1. Mantzavinos D, Kalogerakis N. Treatment of olive mill effluents. Part I: organic matter degradation by chemical and biological processes-an overview. *Environ Int.* 2005; 31(2): 289-95.
2. Komilis DP, Karatzas E, Halvadakis CP. The effect of olive mill wastewater on seed germination after various pretreatment techniques. *J Environ Manage.* 2005; 74(4): 339-48.
3. Nieto LM, Hodaifa G, Rodr'iguez S, Gimenez JA, Ochando J. Degradation of organic matter in olive-oil mill wastewater through homogeneous Fenton-like reaction. *Chemical Engineering Journal.* 2011.
4. Niaounakis M, Halvadakis CP. Olive-mill Waste Management – Literature Review and Patent Survey. Typothito-George Dardanos, Athens. 2004.
5. Roig A, Cayuela ML, Sanchez-Monedero MA. An overview on olive mill wastes and their valorisation methods. *Waste Management.* 2006; 26: 960-969.
6. Roostaei N, Tezel FH. Removal of Phenol from Aqueous Solutions by Adsorption. *Journal of Environmental Management.* 2004; 70: 157-164.
7. Chen GH, Lei, LC, Yue PL. Wet oxidation of high concentration reactive dyes. *Industrial and Engineering Chemistry Research.* 1999; 38: 1837-1843.
8. Kiril Mert B, Yonar T, Yalilikilic M, Kestioglu K. Pre-treatment studies on olive oil mill effluent using physicochemical, Fenton and Fenton-like oxidations processes *J Hazard Mater.* 2010; 174(1-3): 122-8.
9. İnan H, Dimoglo A, Simsek H, Karpuzcu M. Olive oil mill wastewater treatment by means of electro-coagulation. *Separation and Purification Technology.* 2004; 36: 23-31.
10. Ma P, Xiao C, Li L, Shi H, Zhu M. Facile preparation of ferromagnetic alginate-g-poly(vinyl alcohol) microparticles. *European Polymer Journal.* 2008; 44: 3886-3889.
11. Griffiths P, De Hasseth JA. *Fourier Transform Infrared Spectrometry* (2nd ed.). Wiley-Blackwell. ISBN 0. 2007; 471-19404-2.
12. Hasanpour A, Niyafar M, Asan M. Synthesis and Characterization of Fe₃O₄ & ZnO Nanocomposites by Sol- Gel Method, Proceedings of the 4th International Conference on Nanostructures. (ICNS4) 12-14 March, Kish Island, I.R. Iran. 2012.
13. Manouchehr N, Mehriana A, Reza L, Mohammad HR. The optimum conditions for synthesis of Fe₃O₄/ZnO core/shell magnetic nanoparticles for photo degradation of phenol. *J Environ Health Sci Eng.* 2014; 12(1): 21.
14. Vohra MS, Selimuzzaman SM, Al-Suwaiyan, MS. NH₄⁺ -NH₃ removal from simulated wastewater using UV-TiO₂ photocatalysis: effect of co-pollutants and pH. *Environmental Technology.* 2010; 31(6): 641-654.
15. Nassar NN. Iron oxide nanoadsorbents for removal of various pollutants from wastewater: an overview. A. Bhatnagar (Ed.), *Application of Adsorbents for Water Pollution Control*, Bentham Science Publishers. 2012.
16. Anandan S, Vinu A, Venkatachalam N, Arabindoo B, Murugesan V. Photo catalytic activity of ZnO impregnated Hb and mechanical mix of ZnO/Hb in the degradation of monocrotophos in aqueous solution. *Journal of Molecular Catalysis A: Chemical.* 2006; 256: 312-320.
17. Bouallagui Z, Bouaziz M, Lassoued S, Engasser JM, Ghoul M, Sayadi S. Hydroxytyrosol Acyl Esters: Biosynthesis and Activities. *Appl Biochem Biotechnol.* 2011; 163(5): 592-9.
18. Samuel SM, Thirunavukkarasu M, Penumathsa SV, Paul D, Maulik N. Akt/FOXO3a/SIRT1-mediated cardioprotection by tyrosol against ischemic stress in rat in vivo model of myocardial infarction: switching gears toward survival and longevity. *J Agric Food Chem.* 2008; 56(20):